Journal of Communications Technology and Electronics, Vol. 47, No. 7, 2002, pp. 790–795. From Radiotekhnika i Elektronika, Vol. 47, No. 7, 2002, pp. 874–880.

RADIO PHENOMENA IN SOLIDS AND PLASMA

Light Self-Confinement in Planar Cells with Nematic Liquid Crystals[1]

M. Peccianti*, G. Assanto*, A. De Luca, C. Umeton**, M. A. Karpierz***, and I. C. Khoo******

** National Institute for the Physics of Matter &. Dept. of Electronic Engineering Terza University of Rome, Via della Vasca Navale 84, 00146 Rome-Italy*

Tel.: +39 0655177028; Fax no: +39 065579078

E-mail: Assanto@ele.uniroma3.it

*** National Institute for the Physics of Matter & Department of Physics University of Calabria, 87036 Rende (CS)-Italy*

**** Faculty of Physics, Warsaw University of Technology, Koszykowa 75, 00662 Warsaw-Poland*

***** Department of Electrical Engineering, Pennsylvania State University, University Park, Pennsylvania 16802-USA*

Received July 17, 2000

Abstract—Three-dimensional spatial solitons are generated by a linearly-polarized Argon-ion beam in thick planar cells containing prealigned undoped nematic liquid crystals and subject to an externally applied voltage. Self-confinement of the intense beam and guidance of a weak He-Ne probe at a different wavelength but identical polarization are demonstrated with milliwatt powers and over millimeter distances.

Spatial solitary waves or solitons, i.e., cw eigensolutions of a nonlinear system encompassing an intensity-dependent refractive index, have been investigated in a variety of configurations because of their fundamental relevance in physics and, moreover, in optics [1]. More recently, their potential applications for signal readdressing in all-optically reconfigurable interconnects and light-controlled switching have been underlined in various media exhibiting Kerr, photorefractive and quadratic nonlinear responses [2]. After the pioneering work by Braun *et al.* [3, 4] spatial self-confinement of light was experimentally investigated in dye-doped nematic liquid crystals (NLC) by Warenghem *et al.* in NLC filled capillaries [5, 6] and by Karpierz *et al.* in planar cells with homeotropically aligned NLC [7]. Such attention to NLC stems from the reorientational origin of their nonlinearity, which turns out to be wavelength independent and several orders of magnitude greater than in CS_2 [8]. The latter feature allows the observation of a rich phenomenology despite a relatively slow response [9]. NLC, however, are often hampered by a finite propagation length due to scattering and absorption. For this reason, in previous experiments for the observation of self-focusing and spatial solitons, significant attention was devoted i) to lower the required optical power as determined by the so-called Fréedericks transition and ii) to reduce thermal contributions to the nonlinear phenomena. To such extents, external cooling (point ii) was employed by Braun and coworkers in the presence of excitations as large as 10 W in order to observe filamentation [3], dye doping was used in [5] to enhance the nonlinear optical response (point i), while a hybrid (TE/TM) field polarization (point i) was launched in thin homeotropic NLC cells by Karpierz and collaborators in [7]. Nevertheless, in all cases self-confinement was observed over short distances (hundreds of μm) and often with dominant thermooptic contributions [6]. The latter, although not significantly slower than the reorientational response, undermines the polarization selectivity of the phenomenon. Finally, in NLC the liquid-crystalline nature of the molecular medium and its finite viscosity are often the cause of a non-negligible depolarization of the light entering through the input air/NLC interface, often affected by an initial, and rather uncontrolled, molecular misalignment in an otherwise uniaxial or biaxial crystal [9].

In this work, in solving the issues pointed out above, we describe a novel approach towards the observation of fully self-confined spatial solitons in thick planar NLC cells: (a) we employ undoped NLC to reduce the overall optical absorption and the inherent thermal contribution, (b) we apply an external voltage to introduce a pre-tilt of the NLC molecules and -in doing so- eliminate the threshold inherent to the Fréedericks transition and lower the power levels required by the nonlinear phenomenon, (c) we adopt a planar geometry with thick cells in order to exploit the three-dimensionality

[1] This article was submitted by authors in English.

of the solitary solutions, and (d) define and control the input interface in order not to alter the polarization of the exciting field. The use of undoped NLC allows to lower the intrinsic optical absorption and increase the useful propagation distance, nevertheless limited by scattering losses through impurities and refractive disuniformity, i.e., Rayleigh scattering. As the scattering becomes the main source of attenuation, thermal problems are correspondingly reduced, allowing the observation of purely reorientational effects. As far as the voltage is concerned, it forces the NLC molecular dipoles to tilt with respect to their initial position. The latter is guaranteed by the NLC anchorage, planar with reference to the walls defining the cell, and with axes along the propagation direction of the optical beam. When employing an optical field linearly polarized and perpendicular to the walls and the propagation direction (see below), the NLC dipoles are also perpendicular to the field vector, thereby giving rise to a threshold effect in the reorientational response. Such power level, called Fréedericks threshold, can be too high to prevent undesired thermo-optic phenomena. An external (low frequency) voltage induces a dipolar interaction able to tilt the elongated NLC molecules at a nonzero (non $\pi/2$) angle to the direction of propagation (optical electric field), effectively eliminating the afore-mentioned threshold and therefore permitting the use of lower powers, i.e., intensities <50 W/cm^2, [8, 9]. A planar geometry with thickness well exceeding the transverse dimensions of the optical beam is crucial in testing the formation of 3D solitary waves or self-waveguides, whereas one of the lateral coordinates would be eliminated in a thin cell, such as that investigated by Karpierz *et al.* in [7]. The planarity of the geometry, in addition, simplifies the application of a uniformly intense external voltage and the anchoring of the NLC molecules to the confining walls. Finally, an input glass interface with similar anchoring properties to the walls ensures a well-defined transition of the NLC molecular orientation towards its steady alignment far from the boundaries. For an optical field oscillating in the principal plane defined by the direction of propagation and the normal to the cell (top and bottom) boundaries, such arrangement allows the E-vector to remain linearly polarized and perpendicular to the glass walls.

After proper anchoring, the NLC can be modeled as a birefringent medium with orientation locally described by a unit vector or *director*, the spatial distribution of which is governed by elastic forces in the presence of boundary conditions. In particular, our NLC behaves as a positive uniaxial: when a linearly polarized beam propagates in it, it determines a torque, which tends to realign the director parallel to the *E*-field. Considering equal Frank constants *K* for splay, bend and twist of the molecules [8, 9], a coherent light beam of slowly varying envelope $A = A(z)$, and directors free to rotate in the *xz* plane defined by the optic axis and the *E*-field vector, the tilt $\hat{\theta} = \theta(A) - \theta_{rest}$ with respect to the director orientation at rest θ_{rest} can be described by:

$$4K\left(\frac{\partial^2\hat{\theta}}{\partial x^2} + \frac{\partial^2\hat{\theta}}{\partial y^2}\right) + \varepsilon_0\varepsilon_a|A|^2\sin 2(\hat{\theta} + \theta_{rest}) = 0, \quad (1)$$

with x and y the transverse coordinates and $\varepsilon_a = n_e^2 - n_0^2$ the (linear) birefringence. When an additional low-frequency field is effective in the narrow region where the beam travels, the remaining distribution is uniformly altered wherever the nonlinear interaction takes place, with

$$\theta_{rest}(z, V) = \theta_0(V) + [\theta_{in} - \theta_0(V)]\exp(-z/\bar{z}). \quad (2)$$

$\theta_0(V)$ being the distribution due to the external voltage far from the input, θ_{in} the director orientation at the entrance $z = 0$ and $\bar{z}$ a characteristic relaxation length quantifying the transition region from the input to the steady-state distribution. Finally, the beam amplitude will obey [8, 10]:

$$2ik\frac{\partial A}{\partial z} + \left(\frac{\partial^2 A}{\partial x^2} + \frac{\partial^2 A}{\partial y^2}\right) + k_0^2\varepsilon_a(\sin^2\theta - \sin^2\theta_{rest})A = 0, \quad (3)$$

with $k = k_0\sqrt{n_0^2 + \varepsilon^2\sin^2\theta_{rest}}$ the wavevector. For simplicity, in the numerical integration we assume the latter to be a constant vs. z, i.e., $k \approx k_0\sqrt{n_0^2 + \varepsilon^2\sin^2\theta_0}$. Moreover, we take θ_0 to be zero in the absence of the external bias (i.e., ideal planar alignment) and to saturate to the value $\pi/2$ as the voltage reaches a few Volts for cell thicknesses of the order of 100 μm [9]. The approximations and model (1)–(3) above hold valid provided that the light induced reorientation is small and the optical beam propagates in a narrow region, far from top and bottom cell interfaces (i.e., boundaries). In the weak regime, in fact, the refractive index variation can be described by a Kerr-like model encompassing an angular dependence [9, 10], and for $\theta_0 \ll \pi/2$ the resulting equivalent self-focusing power P_{sf} is much lower than the Fréedericks transition threshold P_F [8, 11] with

$$P_{sf} = \frac{\pi^2 P_F}{2\varepsilon_a k^2\sin^2 2\theta_0}. \quad (4)$$

By numerical integration of eqs. (1) through (3), for the commercial nematic "E7" and taking $\theta_{in} = \pi/2$, injecting a Gaussian beam of linear polarization along *x* and various powers and waists, we verified the consistency of the model and computed the system behavior without the applied bias and in the presence of a voltage-induced director redistribution with $\theta_{in} = \pi/2$. Figures 2a and 2b show the corresponding results for an input power of 3.9 mW and a waist of 3 μm. It is appar-

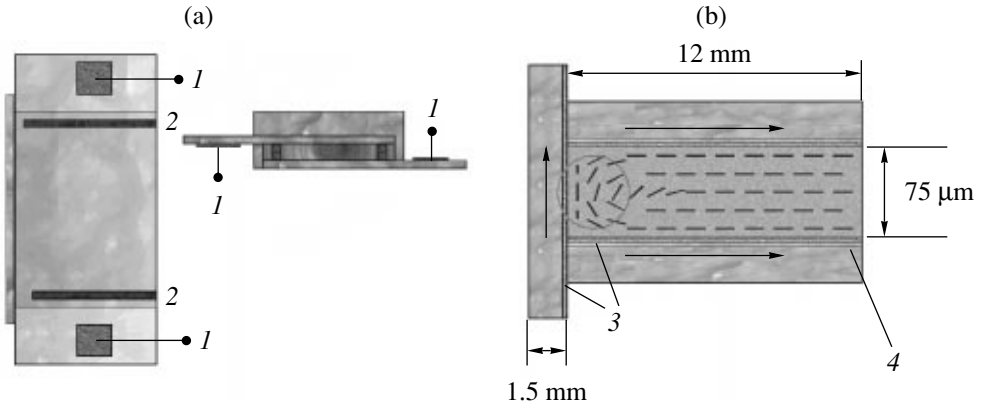

Fig. 1. Schematic of the planar cell containing a properly anchored nematic liquid crystal: (*1*) metal electrodes, (*2*) Mylar spacers, (*3*) Silicon–Oxide film, and (*4*) In–Ta–O electrode.

ent from the simulations that the beam diffracts in the first case (no bias), since no substantial reorientation can take place at excitations below the Fréedericks threshold and, therefore, the resulting propagation is substantially linear (Fig. 2a). Once eliminated the threshold, however, self-focusing can take place and give rise to the formation and propagation of a self-confined solitary wave in the beam-induced refractive index well, as apparent from the contour map of Fig. 2b. Notice that, despite our 2D map representation and in contrast to what expected from a purely Kerr (cubic) response [12], confinement is obtained in both transverse dimensions and is stable due to the saturating nature of the nonlocal nonlinearity.

To verify experimentally our findings and the self-confinement, we fabricated a planar glass cell with Mylar spacers, in order to obtain internal thicknesses of 50–75 μm. Previous to assembling the cell, the glass slides were coated with Indium-Tin-Oxide electrodes for the application of the external voltage, and with Silicon-Oxide to ensure the NLC anchoring with director aligned parallel to the interfaces and along the propagation direction z (Fig. 1). The bias voltage was applied with an AC (1 kHz) sine-wave generator to prevent static effects across the liquid crystal. At the input side of the cell, another pre-treated glass slide (without electrode) was attached to define the $z = 0$ boundary with $\theta_{in} = \pi/2$. The cell was then filled up with the nematic "E7," allowing light propagation over cm distances. The light source was a cw Argon-ion laser, cw emitting at 514 nm and collimated to a waist ≤2.5 μm with a standard 20× microscope objective. The beam, properly attenuated and power monitored, was linearly polarized along x and launched into the NLC cell, well removed from bottom and top glass boundaries. In these samples, no output interfaces were realized to extract the transmitted beam. A Leica optical microscope and a Silicon CCD camera were positioned above the sample to collect the light scattered from the cell and investigate the lightbeam evolution in the y–z plane, as represented in Fig. 3. Additional color and neutral density filters, as well as analyzers, completed the setup and permitted a thorough analysis of the outcoming light.

Figure 4 shows the experimental results for a number of relevant cases, i.e.: (i) at low power (<100 μW), when diffraction dominated (Fig. 4a); (ii) at a power of 6.1 mW and zero bias, when significant self-focusing took place reducing the beam divergence (Fig. 4b); (iii) at a power of 4.2 mW and a 1 V (rms) bias, when the weak light-induced reorientation enabled the formation of a self-confined beam or *spatial soliton*, a beam with z-invariant transverse profile (Fig. 4c). By analyzing the out-of-plane scattered light and its polarization state at low power, as shown in Fig. 5 for the two components, we could estimate $\bar{z} \approx 50$ μm, propagation losses of 5 cm^{-1} and a (full) divergence of nearly 5°, the latter corresponding to a Rayleigh distance of about

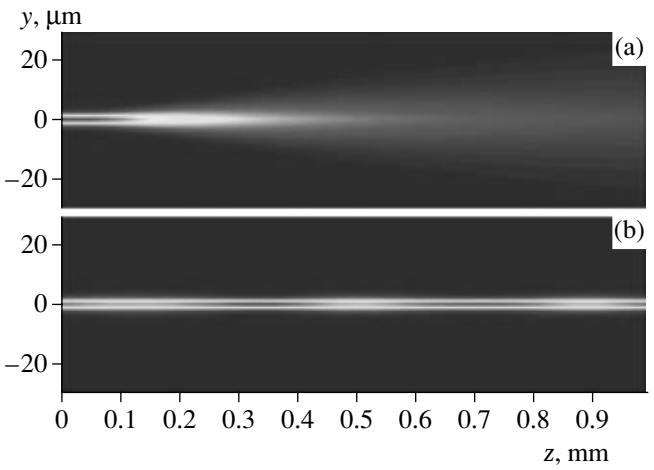

Fig. 2. Numerical simulations from model (1) through (3), with λ = 514 nm, waist = 3 μm, $\bar{z} \cong 40$ μm, input power 3.9 mW, $K = 7 \times 10^{-7}$ g cm/s^2, $\varepsilon_a = n_e^2 - n_o^2 = 0.2$, and (a) zero bias, i.e., $\theta_0 = 0$, (b) nonzero bias, i.e., $\theta_0 = \pi/4$.

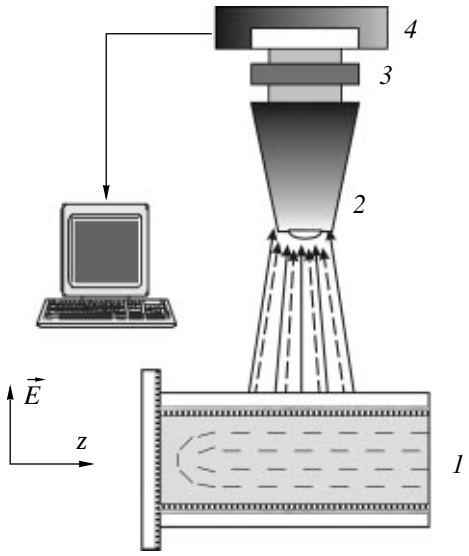

Fig. 3. Sketch of the experimental setup. The cell is properly oriented with an *x*–*y*–*z*–θ stage, and the input beam(s) collimated (along *z*) and linearly polarized in the (*x*–*z*) principal plane.

50 μm. At 4.2 mW, however, within 40 s from the application of a 1 V (rms) bias and after the rearrangement near the interface (z = 0–50 μm), the beam self-confined and propagated diffractionless, as shown in Fig. 4c. At variance with the self-focusing case illustrated by Fig. 4b, in fact, no divergence (diffraction) could be estimated from the acquired data. This behavior is, within experimental errors, the signature of a 3D spatial soliton. It propagated with an unchanged waist over distances in excess of 1.4 mm and essentially limited by the losses.

Since our model and understanding are based on a reorientational nonlinearity, to verify such assumption we performed a number of further experiments at various input (linear) polarizations, excitation levels, bias voltages. The results proved to be always consistent with the model and our interpretation. In particular, a beam polarized along y gave rise to self-focusing (but not *solitons*) only at much higher powers, resulting in additional thermal effects, instabilities and beam breakup. Correspondingly, for a given excitation, strongly focused or defocused input beams led to uncompensated lensing in the cell, with the beam either (initially) converging or diverging. Lower bias voltages were insufficient to modify the director orientation, in a way that the weak optical perturbation could properly compensate. Notice, in fact, that even the electrostatic (low frequency) field has to overcome its own Fréedericks threshold. Finally, exceedingly high biases (well above 1.5 V), while reducing the NLC response time, caused saturation in the director orientation, thereby preventing an effective optical perturbation and the soliton formation.

A *real* index perturbation through a Kerr-like effect should be also sensed by another (polarized) optical beam, and a spatial soliton is expected to create a

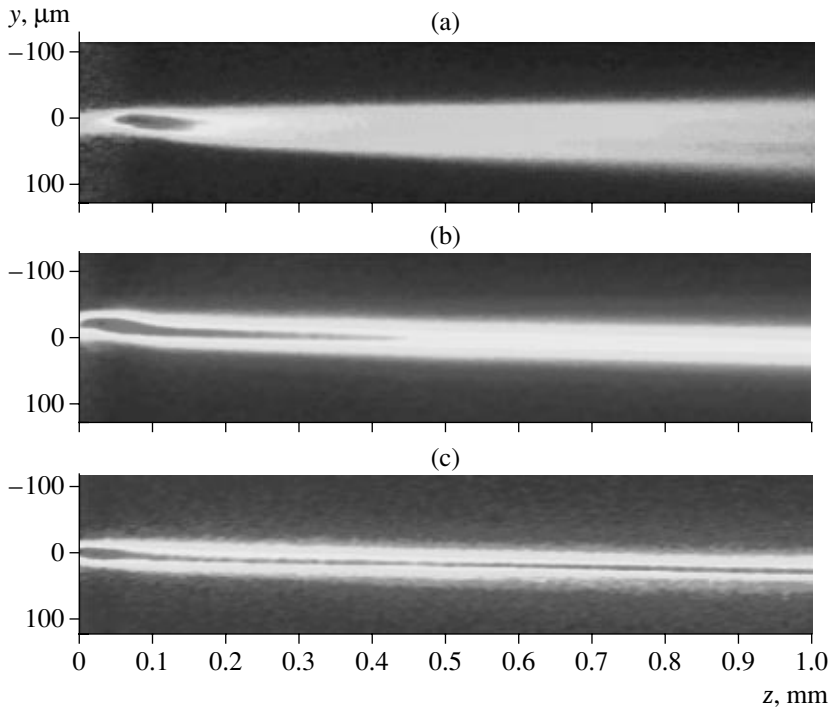

Fig. 4. CCD acquired images of the light scattered from the *x*-polarized Ar^+ beam in the cell: (a) with no external bias and beam power <0.1 mW; (b) no bias and 6.1 mW excitation; and (c) 40 s after applying a 1 V bias at 1 kHz with 4.2 mW input power.

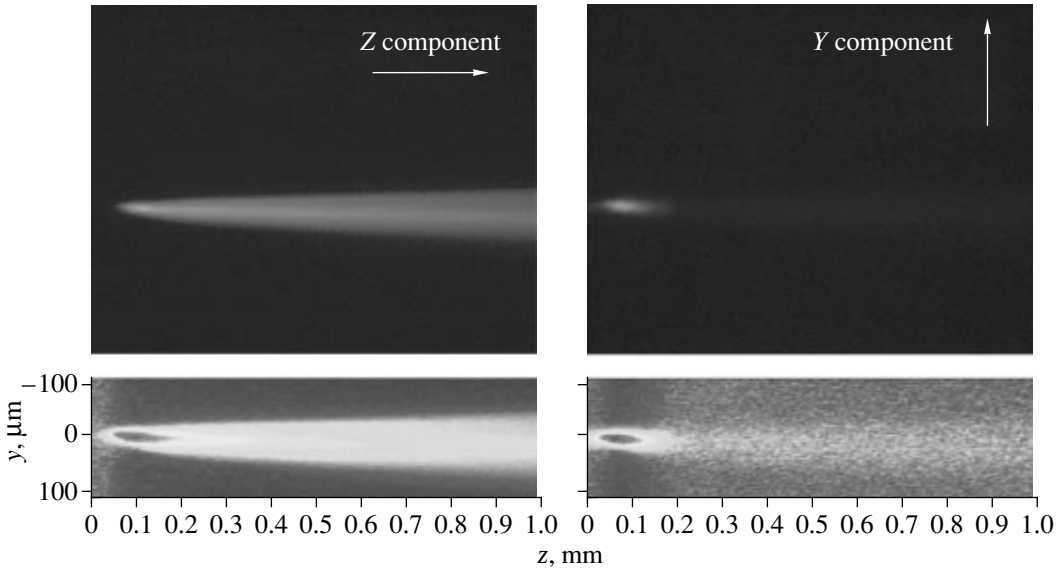

Fig. 5. Out-of-plane scattered beam light and its polarization at low power. From these images, a director-rearrangement distance $\bar{z} \cong 50$ μm can be inferred.

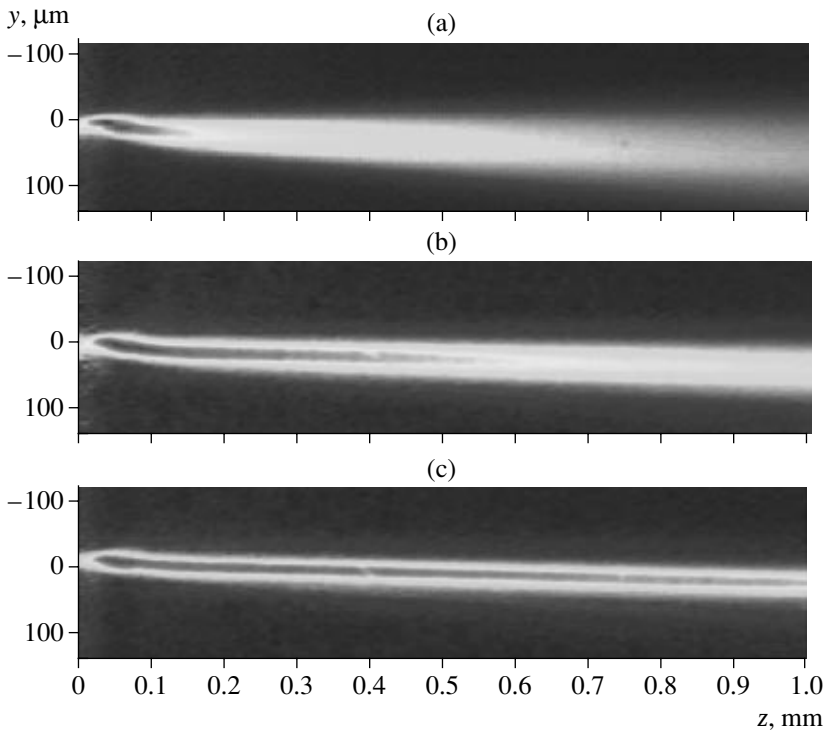

Fig. 6. CCD images of the light scattered from the weak (<0.1 mW) He–Ne laser beam ($\lambda = 633$ nm), co-launched and co-polarized with the Ar^+ pump. The cases (a) through (c) correspond to the excitation conditions in Fig. 4. In (c) the green (Ar^+) soliton writes a channel supporting the guided-wave propagation of the weak probe.

refractive well resulting in transverse light confinement. To ascertain such effects and verify the potential of this phenomenon in routing applications, we co-launched a weak collinear probe beam from a Helium-Neon laser operating at $\lambda = 633$ nm. When it was polarized along *x*, i.e., copolarized with the pump beam at 514 nm from the Argon laser, corresponding to the three cases shown in Fig. 4 we observed the behavior displayed in Fig. 6 (a through c). Specifically, the *x*-polarized He–Ne light consistently followed the pump, and was diffracted (Fig. 6a), focused (Fig. 6b) or guided (Fig. 6c) whenever the pump was diffracted

(Fig. 4a), self-focused (Fig. 4b) or self-guided (Fig. 4c). The latter feature, verified only for *x*-copolarized pump and probe, demonstrates the reorientational (non thermal) origin of the NLC nonlinear response and the formation of an all-optically induced (polarization sensitive) channel waveguide.

The observed solitons, reorientational in nature and polarization sensitive, have transverse size determined by the interplay of the beam size, the NLC elastic s forces and the boundary conditions (anchoring). The two latter factors are such that, even for a laser beam with vanishing waist, the soliton would exhibit a finite width. Temperature and cell thickness, acting on the NLC molecules and their mutual interactions, however, can affect the resulting soliton width even in the presence of a very narrow excitation. In particular, we observed 2–3 times thinner spatial solitons in a 50 μm cell, at 11 mW input power and the same excitation parameters previously employed.

In conclusion, we have observed 3D spatial solitons in voltage-biased and planarly-oriented undoped nematic liquid crystals. These reorientational solitons form and propagate at excitation powers of a few mW and for distances an order of magnitude longer than the diffraction length. Propagating in a positive uniaxial, the solitons are polarization sensitive and able to support the transverse confinement of a copolarized probe signal at a longer wavelength.

Noticeably, since this saturating nonlinearity is nonresonant, the observed phenomena do not depend on wavelength and can also be exploited in the 1.3–1.5 μm spectral region used for optical communications. Such solitons, despite their relatively slow response, could have important implications towards all-optically reconfigurable interconnects, where spatial switching and all-optical logic [13, 14] could also be effectively implemented.

ACKNOWLEDGMENTS

G.A. is indebted to Dr. N. Tabiryan (Beam Engineering Corp., Oviedo, USA), and Prof. G.I. Stegeman (Univ. Central Florida, Orlando, USA), for enlightening discussions. The work in Italy was supported by INFM (contract PRA 2002 on “Transverse localization and optical signal processing via spatial solitons in nematic liquid crystals”).

REFERENCES

1. Segev, M. and Stegeman, G.I., *Phys. Today*, 1998, vol. 51, no. 8, p. 42.
2. *Beam Shaping and Control with Nonlinear Optics*, Kajzar, F. and Reinisch, R., Eds., N.Y.: Plenum Press, 1997.
3. Braun, E., Faucheux, L., Libchaber, A., *Phys. Rev. A*, 1993, vol. 48, no. 1, p. 611.
4. Braun, E., Faucheux, L., Libchaber, A., *et al.*, *Europhys. Lett.*, 1993, vol. 23, no. 4, p. 239.
5. Warenghem, M., Henninot, J.F., and Abbate, G., *Opt. Expr.*, 1998, vol. 12, p. 483.
6. Derrien, F., Henninot, J.F., Warenghem, M., and Abbate, G., *J. Optics A*, 2000, vol. 2, p. 332.
7. Karpierz, A.M., Sierakowski, M., Swillo, M., Wolinski, T., *Mol. Cryst. Liq. Cryst.*, 1998, vol. 320, p. 157.
8. Tabyrian, N.V., Sukhov, A.V., Zel’dovich, B.Y., *Mol. Cryst. Liq. Cryst.*, 1986, vol. 136, p. 1.
9. Khoo, I.C., *Liquid Crystals: Physical Properties and Nonlinear Optical Phenomena*, N.Y.: Wiley, 1995.
10. Herman, R.M. and Serinko, R.J., *Phys. Rev. A*, 1979, vol. 19, no. 4, p. 1757.
11. McLaughlin, D.W., Muraki, D.J., Shelley, M.J., and Wang, Z., *Physica D*, 1996, vol. 97, p. 471.
12. Kelley, P.L., *Phys. Rev. Lett.*, 1965, vol. 15, no. 26, p. 1005.
13. Shi, T.T. and Chi, S., *Opt. Lett.*, vol. 15, no. 15, p. 1123.
14. McLeod, R., Wagner, K., and Blair, S., *Phys. Rev. A*, 1995, no. 4, p. 3254.